

THE KING'S POINT COMPLEX, NEWFOUNDLAND, AND ITS POTENTIAL FOR RARE-METAL MINERALIZATION

R.R. Miller and A.M. Abdel-Rahman¹
Mineral Deposits Section

ABSTRACT

The King's Point complex (KPC) contains a peralkaline volcanic suite, consisting of aphyric to porphyritic comenditic ash-flow tuffs, amphibole-bearing ring dykes, ring fault ash-flow tuffs, and related granophyric hypabyssal rocks, and a hypersolvus peralkaline plutonic suite, dominantly consisting of porphyritic syenite and minor amounts of granite. Metaluminous volcanic rocks, correlated with the Springdale Group, form the floor of the cauldron complex. Late metaluminous granites, associated with regional faults, crosscut the peralkaline suite. Amphibole-porphyrific ring dykes outline at least two calderas and segments of several others, indicating that the complex consists of a number of nested calderas ranging in size from 4 to 10 km in diameter. The southeastern portion of the KPC is missing owing to movement along the Green Bay fault. The widespread occurrence of centrally located porphyritic syenite suggests that it represents a resurgent intrusion.

Mineralogically, the complex contains variable amounts of perthite, quartz, clinopyroxene and amphibole with accessory zircon, apatite, aenigmatite, astrophyllite, chlorite-smectite and titanite. The pyroxenes vary from ferrosillite to hedenbergite to aegirine, whereas the amphibole forms a continuous solid solution series from ferrichterite to arfvedsonite. These sodic-rich mafic minerals formed from Na- and volatile-rich late-stage magmas, indicating that these volcanic rocks originated from a peralkaline magma. Red chlorite-smectite and sericite formed during subsolidus hydrothermal alteration of alkali mafic minerals and feldspars, respectively. The hydrothermal event resulted in reduction in the peralkalinity of initially peralkaline volcanic rocks; however, rare metals were immobile or conserved during this event.

The KPC contains peralkaline volcanic and plutonic members that are potential hosts of rare-metal mineralization (e.g., Zr, Nb, Y). However, significant concentrations and quantities of rare metals are absent; thus, the potential is very low.

INTRODUCTION

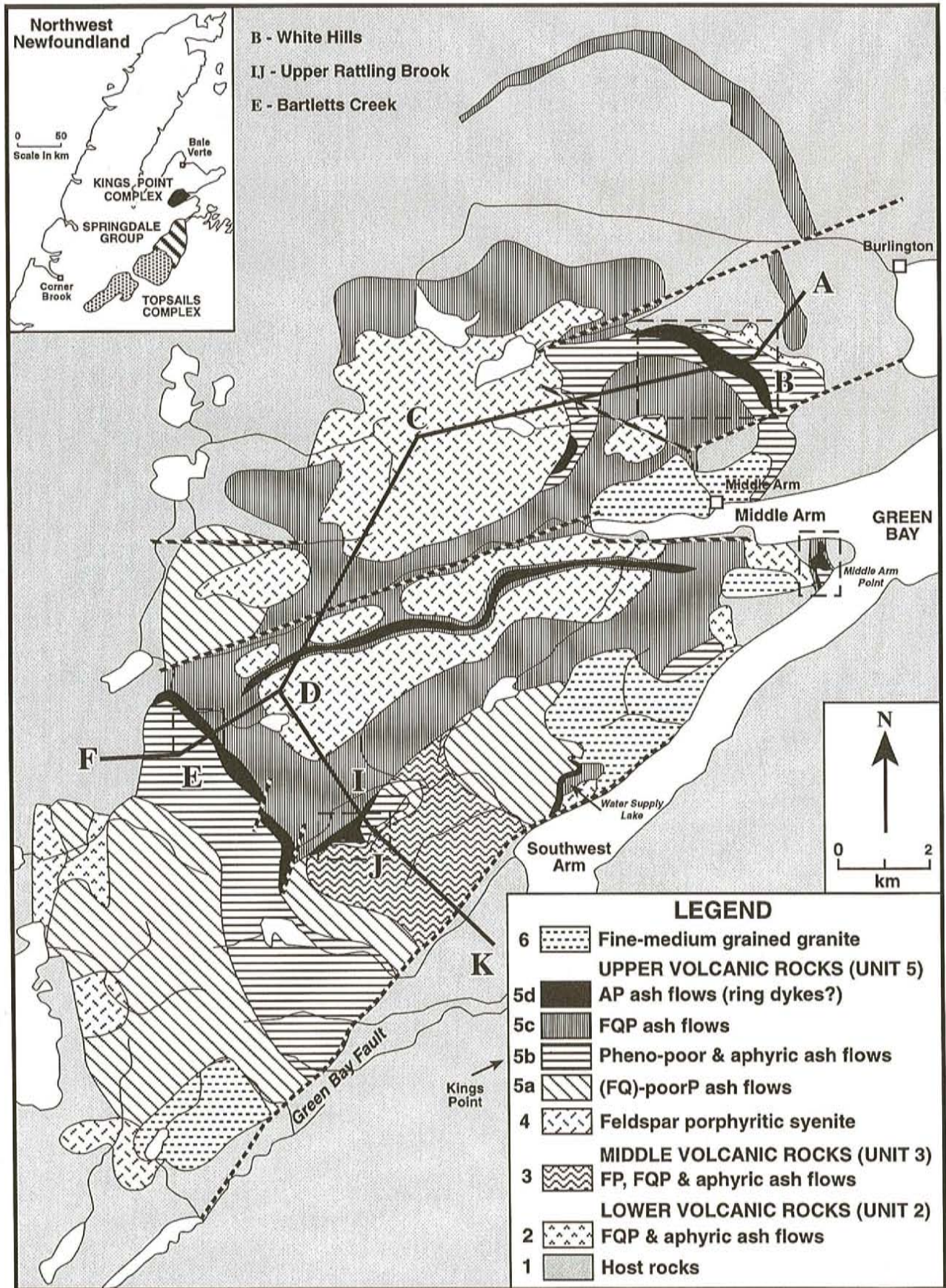
The King's Point complex (KPC—Mercer *et al.*, 1985) consists of Silurian (427 Ma, U-Pb zircon date, Coyle, 1990) peralkaline to metaluminous volcanic, hypabyssal and plutonic rocks, occupying an area of 275 km² on the southeastern Baie Verte Peninsula, near the communities of King's Point, Middle Arm and Burlington (Figure 1). Country rocks mainly consist of Burlington granodiorite (432 ± 2 Ma, Cawood and Dunning, 1993) and lesser amounts of mafic metavolcanic rocks on the northern and western borders, and Lushs Bight Group volcanic rocks on the southeastern border of the KPC (Mercer *et al.*, 1985; Kontak and Strong, 1986).

Silurian magmatic activity in west-central Newfoundland (e.g., Springdale Group and Topsails igneous suite) is late- to post-orogenic, possibly related to subduction under a continental margin (Coyle and Strong, 1987; Whalen, 1989). Several previous studies (e.g., Coyle and Strong, 1987; Whalen *et al.*, 1987b) correlate the KPC with the Topsails

granite and related volcanic rocks (427 and 429 Ma, Whalen *et al.*, 1987b), the Springdale Group (427 Ma, Chandler *et al.*, 1987; 432 Ma, Coyle, 1990), the Cape St. John Group (427 Ma, Coyle, 1990) and the Seal Island Bight syenite (435 to 414 Ma, Hibbard, 1983); collectively, these suites define the Topsails granite association of the western Dunnage Zone (Williams *et al.*, 1989; Fryer *et al.*, 1992).

The KPC is a target with potential for rare-metal mineralization based on the model and interpretation of Miller (1988, 1989, 1991). This model, developed for high-level peralkaline rock-hosted, rare-metal mineralization, contains elements derived from metallogenic studies of the Strange Lake Zr-Y-Nb-Be-REE deposit (Miller, 1986), the Mann-Type Nb-Be ± Y showings in the Letitia Lake area (Miller, 1987; Batterson and Miller, 1987), the undersaturated phases of the Red Wine Alkaline Intrusive Suite (Miller, 1988) and ash-flow tuff-hosted mineralization in the Flowers River cauldron complex (Miller, 1988, 1992, 1993; Miller and Abdel-Rahman, 1992; R.R. Miller and A.M. Abdel-Rahman,

¹ Department of Geology, Concordia University, 7141 Sherbrooke Street West, Montreal, Quebec, Canada, H4B 1R6



unpublished data). Rare-metal mineralization (i.e., containing one or more of Zr, Y, REE, Nb, Ta, Be) occurs in dominantly felsic peralkaline and near-peralkaline anorogenic intrusions, and their near-vent extrusive equivalents (Miller, 1988, 1991); in addition, the highest grades of mineralization occur in low-volume, late-stage differentiates such as pegmatite–aplite dykes, roof-zone magmas and thin ash-flow tuffs.

As part of an evaluation of rare-metal potential, this report outlines the following features of the KPC: 1) the stratigraphy of the volcanic units; 2) major aspects of the structure and geology; and 3) the chemostratigraphy of the volcanic units and representative geochemistry of the intrusive units. Preliminary mapping and geochemical studies (Miller, 1991) identified a unit of peralkaline amphibole-bearing ash-flow tuffs as the best rare-metal target in the KPC; accordingly, this manuscript focuses on the geochemistry, setting and mineralogy of this unit and surrounding rocks.

GEOLOGY AND STRATIGRAPHY

The KPC consists of a sequence of felsic subaerial ash-flow tuffs, which are at least 900 m thick, and a suite of felsic hypabyssal to subvolcanic intrusive rocks (Mercer *et al.*, 1985, Kontak and Strong, 1986). The Green Bay fault (Hibbard, 1983) defines the southeastern border of the KPC. Figure 1 illustrates the generalized geology of the KPC as compiled from Mercer *et al.* (1985), Kontak and Strong (1986), Prior (1988) and this study. The legend in Figure 1 displays the stratigraphy of the volcanic rocks in the complex and Figure 2 displays interpretive southwest–northeast and southeast–northwest cross-sections.

The intrusive rocks of the KPC exhibit variable textures and compositions; however, the two main phases are feldspar±quartz-porphyritic syenite (Unit 4), and fine- to medium-grained granite (Unit 6). Rare contact relationships between the porphyritic syenite and peralkaline dykes suggest that the syenite is older than the upper volcanic unit (Unit 5). The occurrence of fine- to medium-grained granite along post-KPC faults (Figure 1), and the presence within it of rare xenoliths of volcanic rocks, suggest that these granites are the youngest unit observed in the complex; furthermore, they suggest that these granites are genetically unrelated to the other units.

Field and geochemical data divide the volcanic rocks into three units and several subunits: Lower, Middle and Upper units (Units 2, 3 and 5). Unit 2 consists of over 50 m of white aphyric to quartz-feldspar-porphyritic ash-flow tuff, lapilli tuff and breccia. Unit 3 contains over 200 m of beige to red aphyric to quartz-feldspar-porphyritic ash-flow tuffs and breccias. Unit 5 comprises at least 700 m of aphyric to

sparsely porphyritic ash-flow tuffs (subunits 5a,b), quartz-feldspar±amphibole-porphyritic ash-flow tuffs and intrusive equivalents (subunit 5c), and amphibole-bearing ash-flow tuffs (subunit 5d).

UNIT 2 (LOWER VOLCANIC UNIT)

Aphyric to quartz-feldspar-porphyritic ash-flows of this stratigraphically lowermost unit form small outcrop areas and occur throughout the complex. They occur in a well-defined unit in the northeastern part of the KPC and in scattered occurrences in the south-central and southern part of the complex (Figure 1). Outcrop distribution is difficult to establish without field relationships and geochemical data, because tuffaceous members of Unit 2 are indistinguishable in outcrop from some members of Unit 3 and 5; also, faulting complicates the stratigraphy of the south-central occurrences.

In the northeastern occurrence, Unit 2 is dominantly a quartz-feldspar-porphyritic ash-flow tuff to breccia consisting of up to 40 percent fragments, which range in size from <1 to 30 cm. Fragments consist of subangular to subrounded aphyric flows and quartz-feldspar porphyry or granite (Burlington granodiorite?). The south-central occurrence is a plagioclase, K-feldspar and quartz-porphyritic ash-flow tuff.

UNIT 3 (MIDDLE VOLCANIC UNIT)

Strata of this unit outcrop over an area of 15 km² (6 percent) in south-central KPC (Figure 1). They vary in texture, ranging from aphyric to sparsely porphyritic, to porphyritic and lithophysae-bearing ash-flow tuffs, ash-flow lapilli-tuffs and breccias. Contact relationships are absent; however, chemostratigraphic data and comparison with the Springdale Group (see Discussion section) indicate a genetic relationship with Unit 2 and suggest that Unit 5 is younger.

Sericite, hematite and silica alteration of these rocks are common (Prior, 1988; *this study*); carbonate and epidote are also common secondary minerals. Plagioclase is the most common feldspar. Lithic breccias mainly consist of aphyric fragments in an aphyric ash-flow tuff matrix.

UNIT 4 (FELDSPAR±QUARTZ-PORPHYRITIC SYENITE)

This intrusive unit occupies approximately 25 percent (≈ 65 km²) of the present outcrop of the KPC and occurs as one large, irregularly shaped, body with a series of satellite bodies, located in the north-central part of the complex, and three small bodies in the southern part (Figure 1). It ranges from feldspar-porphyritic syenite to feldspar±quartz-

Figure 1. General geology of the King's Point complex, including location insert-map and cross-section line locations of Figure 2; geology after Mercer *et al.* (1985), Kontak and Strong (1986), Prior (1988), and Miller (unpublished map). This map also indicates the locations of the more detailed maps in Figure 3. Abbreviations in legend are: A = amphibole, F = feldspar, Q = quartz, P = porphyritic.

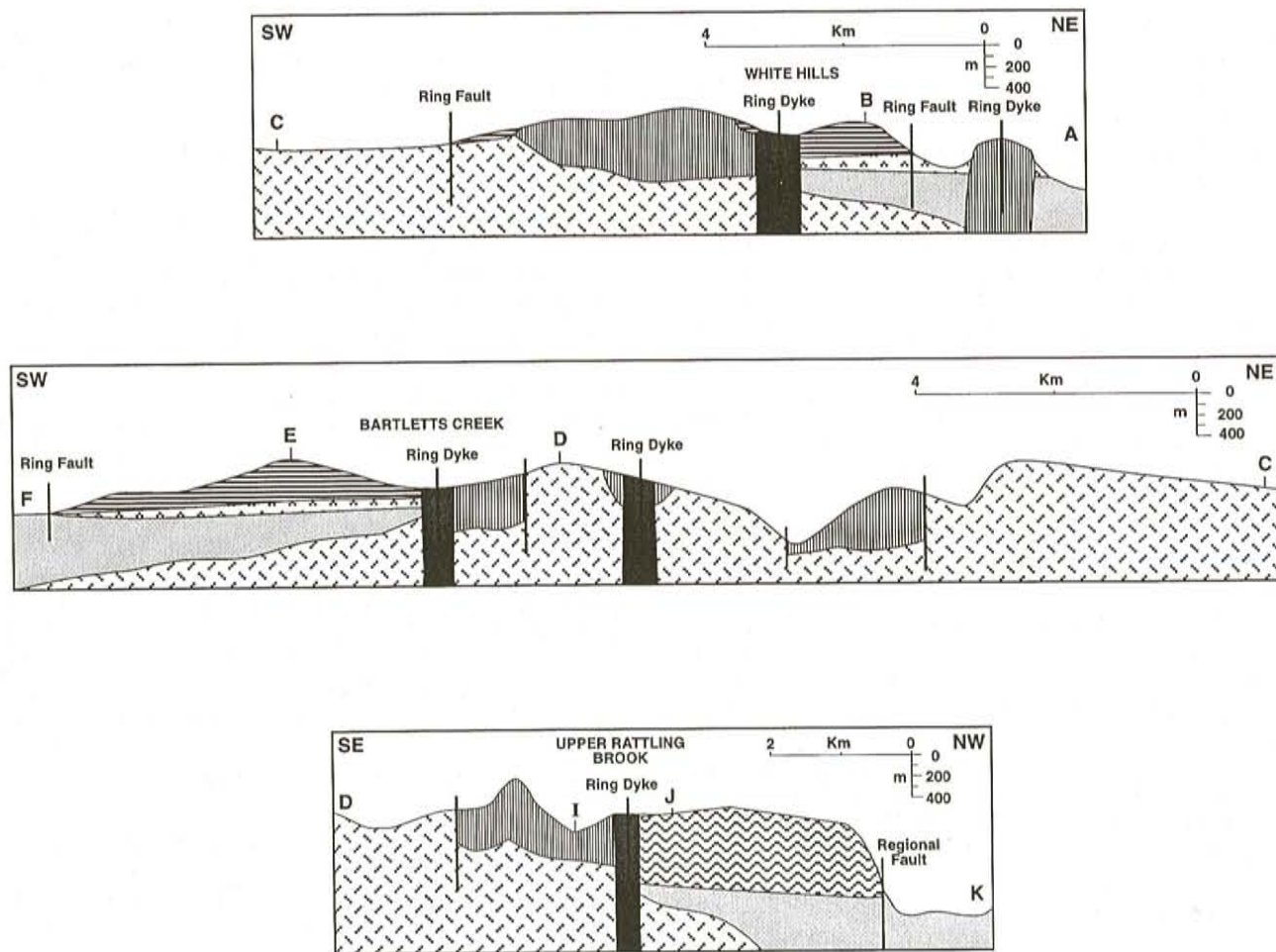


Figure 2. Generalized interpretive cross-sections through the King's Point complex; sections are located in Figure 1. Note that section A-B-C and C-D-E-F join at location C to form a single cross-section extending from the northeast to the southwest.

porphyritic quartz syenite and granite (also see Kontak and Strong, 1986), with less common equigranular variants. It usually contains <5 percent rounded to subrounded fine-grained mafic inclusions (<5 cm across; rarely up to several metres in size).

This unit characteristically contains 10 to 30 percent subhedral feldspar phenocrysts, which range in size from 3 to 10 mm. Micropertite commonly occurs as the dominant feldspar along with subordinate numbers of plagioclase grains. Up to 5 percent quartz phenocrysts, less than 4 mm in diameter, sparsely occur in some outcrops. The groundmass commonly exhibits granophyric and graphic granite-textured quartz and feldspar with accessory magnetite, pale clinopyroxene (ferrosilite) and amphibole. Inclusions are usually very fine grained, but rare coarser grained inclusions contain plagioclase and clinopyroxene.

UNIT 5 (UPPER VOLCANIC UNIT)

The members of this unit occupy almost 60 percent of the KPC (Figure 1; 162 km²). They vary in texture, ranging from aphyric to sparsely porphyritic (subunits 5a, b), to

porphyritic (subunits 5c, d), to fine-grained hypabyssal equivalents. All outcrops of extrusive rocks display an aphyric groundmass and appear to be mostly ash-flow tuffs and ring-dyke units. In outcrops where amphibole is absent in subunit 5b, chemostratigraphic data distinguish phenocryst-poor ash-flow tuffs of subunits 5a and 5b. Crosscutting ring dykes and related ash-flow tuffs of subunit 5d indicate that this unit is younger than subunits 5b and 5c. Stratigraphic data suggest that subunit 5a occurs above Unit 3; thus, it is older than subunits 5b and 5d.

Subunit 5a occurs on the western and eastern borders of the complex. In the north, it occurs with subunit 5c, and in the south it occurs with subunit 5b. Subunit 5a exhibits many of the textures and rock types of subunit 5b; however, geochemical contrast and local stratigraphic relationships distinguish between these units.

Ash-flow tuffs of subunit 5b occur in two main areas (Figure 1), an arc-shaped body in the northeast (White Hills area) and an elongate area in the south (Bartletts Creek area); three smaller areas occur on the southeastern margin of the KPC. These comprise aphyric to phenocryst-poor (5 to 10)

percent) ash-flow tuffs having an aphanitic groundmass; phenocryst-rich ash-flow tuffs sparsely occur. Microperthitic feldspar is the most common phenocryst (up to 20 percent), whereas quartz (3 to 15 percent) and amphibole (up to 15 percent) are less abundant. Phenocrysts range from 1 to 4 mm in size and broken phenocrysts are common. The groundmass is usually recrystallized and exhibits ash-flow textures such as fiamme and layering.

Subunit 5c consists of quartz-feldspar-porphyrific ash-flow tuffs and breccias and possible hypabyssal intrusive equivalents. This unit forms a partial ring surrounding the northern body of Unit 4 porphyritic syenite and an almost complete ring around Unit 4 bodies in the central part of the KPC. The northern, outlying, ring dyke of the KPC also mainly consists of subunit 5c; small bodies also occur, associated with ring dykes, on the southeastern margin. The total estimated thickness is 600 m and total area is 24 km². Subunit 5c characteristically contains 20 to 35 percent microperthitic feldspar and 5 to 15 percent quartz phenocrysts from 1 to 4 mm across. Oikocrystic amphibole, anhedral amphibole and rarely clinopyroxene occur as grains up to 1 mm across and in quantities up to 5 percent. Broken crystals, resorbed quartz, fiamme and compaction features indicate that most occurrences are ash-flow tuffs. Kontak and Strong (1986) favour an intrusive or gradational contact relationship between part of subunit 5c and the older Unit 4; however, geochemical (see below) and textural data argue against this interpretation.

Subunit 5d (Ring Dykes)

Amphibole-bearing ash-flow tuffs (subunit 5d; outlined separately in Figure 1) were the focus of detailed follow-up work in the KPC because of their good potential for rare-metal mineralization. Detailed sampling and mapping focused on the Bartletts Creek, Upper Rattling Brook, Water Supply Lake, Middle Arm Point and White Hills areas; Figure 3 illustrates the geology of four of these areas. Subunit 5d ash-flow tuffs form at least two partial ring structures in the White Hills and Bartletts Creek areas; smaller ring segments occur in the Middle Arm Point, Upper Rattling Brook and Water Supply Lake areas and a larger linear segment occurs on the southern flank of Middle Arm (Figure 1). All of these areas generally contain the same textural varieties of subunit 5d, although the arrangement of these varieties, the attitude of the bedding and the relationships with the nearby units are variable.

The amphibole-porphyrific ash-flow tuffs (subunit 5d) characteristically contain oikocrystic phenocrysts or aggregates of black amphibole. They range from highly welded and compacted, layered, ash flows through more massive oikocrystic amphibole and red-spotted ash flows, to massive or layered aphyric flows having fine-grained amphibole and aegirine microphenocrysts in the groundmass. Amphibole commonly occurs as grains up to 1 mm in size, which occur in aggregates or as oikocrystic grains and aggregates of grains up to 2 mm across. Aegirine is commonly subhedral and occurs as single grains up to 0.2 mm across.

Quartz and feldspar phenocrysts are sparse. Ash-flow textures commonly occur in most occurrences. The red spots observed in outcrop appear to be zones of very fine-grained secondary hematite in the matrix, which may be pseudomorphing an unknown mineral.

Large thicknesses, up to 350 m, of aphyric to sparsely porphyritic ash-flow tuffs (subunit 5b) occur with the amphibole-bearing ash flows (subunit 5d) in the White Hills and the Bartletts Creek areas; smaller thicknesses (commonly < 10 m) occur at the Upper Rattling Brook and Water Supply Lake occurrences. These occurrences commonly display fiamme and compaction features characteristic of ash-flow tuffs; sparse very fine amphibole grains also occur in some outcrops. Stratigraphic relationships indicate that these ash flows are generally lower in the stratigraphy than the occurrences of subunit 5c.

Most occurrences of subunit 5d are mainly moderately to highly welded ash-flow tuffs having abundant features confirming a pyroclastic flow origin. Highly flattened, intensely stretched and welded glass shards (Plate 1) showing well-developed eutaxitic, as well as axiolytic textures, and the common presence of spherulites are obvious devitrification textures. Recrystallization, then coarsening of devitrified glass shards and groundmass materials, perlitic fractures, and the presence of fragmented (broken) phenocrysts, also are typical ignimbritic textures, and reflect the tuffaceous nature of these volcanic rocks. Finely laminated (banded) tuff is common; it occurs as white bands alternating with greenish bands, white bands in a black matrix, or black bands in a reddish matrix.

Contact relationships in the Middle Arm Point, Water Supply Lake and the Upper Rattling Brook areas indicate that subunit 5d intrudes overlying quartz-feldspar-amphibole-porphyrific ash-flows (subunit 5c); however, there are apparently gradational contacts between subunit 5d and subunits 5b and 5c in the White Hills and the Upper Rattling Brook areas. In many localities, subunit 5d dips very steeply (50 to 90 percent, Figure 3). These contact, stratigraphic and other relationships suggest that many of the amphibole-bearing ash flows form within a ring dyke or near the vent site of a ring-fault system. These locations should contain the products of low-volume eruptions with the highest potential for rare-metal mineralization. Similar textures and contact relationships occur in the amphibole-bearing ring dykes of the Flowers River cauldron complex (Miller, 1992, 1993; Abdel-Rahman and Miller, 1993; R.R. Miller and A.M. Abdel-Rahman, unpublished data), although rare-metal mineralization rarely occurs in the ring dykes of this complex.

UNIT 6 (FINE- TO MEDIUM-GRAINED GRANITE)

This unit occurs as four small bodies, ranging in size from 1 to 9 km², which occur along the eastern contact of the KPC (8 percent of the KPC). The two southerly and the most northerly bodies mostly contain massive fine-grained granite with subordinate medium-grained granite. The other body mainly consists of medium-grained granite. The fine-grained granite contains rare very fine-grained mafic

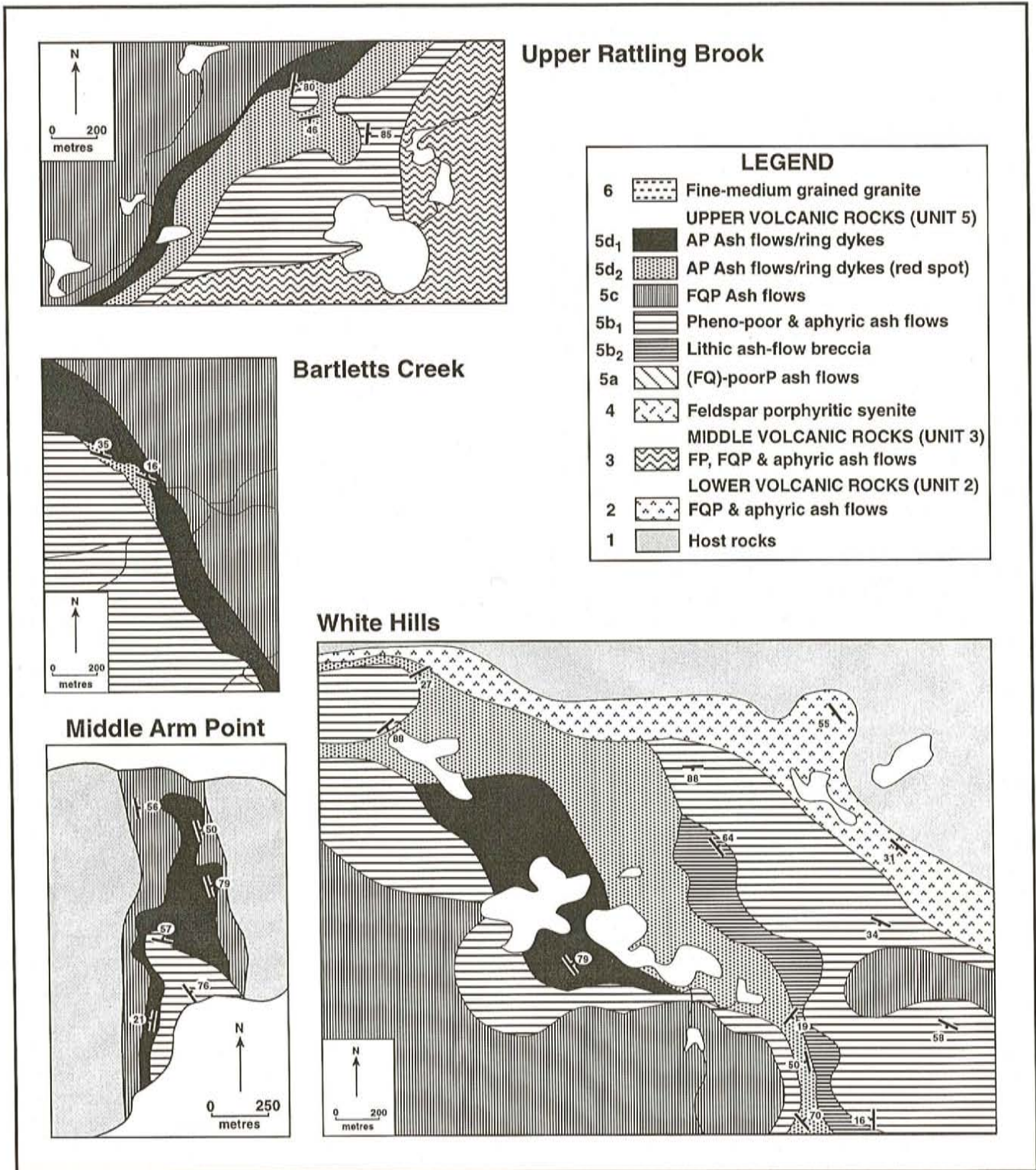


Figure 3. Detailed geology of four segments of amphibole-bearing ring dykes and ring-dyke volcanic rocks in the King's Point complex. White Hills, Bartletts Creek and Upper Rattling Brook localities are located in the cross-sections of Figure 2; Middle Arm Point is located on the northeastern edge of the KPC between Middle Arm and Southwest Arm. Abbreviations used in the legends are: A = amphibole, F = feldspar, Q = quartz, P = porphyritic.



Plate 1. Photograph of highly flattened and welded amphibole ash-flow tuff (subunit 5d) from the Bartletts Creek ring-dyke locality.

inclusions similar to those found in Unit 4. In one locality, Unit 6 contains inclusions of quartz-feldspar porphyry (Unit 5); thus, Unit 6 is younger than Unit 5.

The fine-grained granite consists of 75 to 95 percent feldspar, commonly less than 2 mm in size, less than 5 to 25 percent quartz up to 3 mm in size, and 3 to 8 percent amphibole less than 1 mm in size. Feldspar occurs as single grains of micropertthite and plagioclase or in massive granophyric/graphic granite-textured quartz-feldspar intergrowths. In some outcrops, phenocrysts of either micropertthite or plagioclase or both occur in a granophyric matrix. Spherulitic textures are rarely present.

STRUCTURE

The suggestion that the KPC is a ring complex associated with caldera collapse (Hibbard, 1983 and references therein; Mercer *et al.*, 1985; Coyle and Strong, 1987) is consistent with the results of this study. However, the newly defined volcanic stratigraphy and ring-dyke systems indicate that the KPC consists of several nested calderas, and possibly a central resurgent intrusion and that its overall structure is complex.

Amphibole-bearing ash flows and dykes of subunit 5d define ring-dyke systems inferred to outline individual calderas. These indicate at least one partial caldera in the White Hills area (5 x 4 km), one in the Bartletts Creek area (4 x 4 km) and the segments of others in the Middle Arm Point, the central and Water Supply Lake areas. The large ring dyke at the northern end of the complex may also outline another caldera, which must have been at least 10 x 10 km in dimension. The position of Unit 4 feldspar-porphyrific syenite in a central part of the complex suggests that this intrusion represents either a resurgent intrusion or the roof zone of one or more intrusions parental to the downfaulted volcanic rocks.

Unit 6 syenite and granite occur as small intrusions located on or near the Green Bay fault and may represent

younger rocks associated with the fault-forming tectonic activity. Other post-caldera faults offset the volcanic stratigraphy (Figure 1); a large fault occurs in Middle Arm and along Middle Arm Brook. Lateral movement along the Green Bay fault may be as much as 50 km (Coyle and Strong, 1987), whereas movement along the other faults is probably less than a few kilometres. The termination of the Middle Arm and Water Supply Lake ring dykes at the Green Bay fault indicates that parts of the KPC occur elsewhere. The structural interpretation of Coyle and Strong (1987) indicates that the Sheffield Lake group (Coyle *et al.*, 1986), which contains amphibole-bearing peralkaline volcanic and subvolcanic rocks, is the missing portion of the KPC.

MINERALOGY

The plutonic and volcanic rock units are composed of variable amounts of feldspars, quartz, alkali amphibole, iron-rich clinopyroxene and sodic pyroxene, accessories and opaque phases. Mineral compositions were obtained on polished thin sections, which were vacuum-coated with carbon, using the computerized Camebax electron microprobe at McGill University. The probe was operated using the wavelength-dispersion mode (WDS) with an accelerating voltage of 15 kV, and a beam current of 5 Å (for details of analytical techniques, see Abdel-Rahman, 1992). Representative chemical compositions of the various phases analyzed, and their calculated structural formulae, are presented in Table 1.

Feldspar is the main mineral phase in all plutonic varieties and is mostly present as one phase (perthite), thus reflecting the hypersolvus nature of this suite. Exsolution has produced near end-members, albite and K-feldspar, as shown by the composition of the lamella and host, respectively (Table 1). Perthite is the earliest rock-forming mineral to crystallize in most plutonic rocks of this complex.

Quartz occurs in graphic intergrowth with feldspars, as a phenocryst showing the square cross section of β -quartz in porphyritic varieties, or in a micro- to cryptocrystalline mosaic (along with feldspar) in groundmass materials and devitrified shards and spherules.

Pyroxene is represented by iron-rich, Na-bearing varieties. Such clinopyroxene is commonly rimmed by aegirine or alkali amphibole. Aegirine may also occur as subhedral to euhedral, poikilitic (rarely oikocrystic), strongly pleochroic crystals. Clinopyroxene varies in composition (Table 1) from ferrosilite, hedenbergite (containing an acmitic component) to near end-member aegirine (Figure 4). Extensive solid solution between hedenbergite and aegirine is illustrated in Figure 4. The evolutionary (Na-enrichment) trend observed here is comparable to those from several other suites (e.g., Platt and Woolley, 1986; Azambre *et al.*, 1992).

Amphibole is typically highly pleochroic and varies from bluish green to brownish green, characteristic of alkali amphibole. It occurs as large euhedral crystals in syenite and granite (Units 3, 4, and subunit 5c) and as oikocrysts with

Table 1. Representative analyses and structural formulae of minerals from the King's Point complex

	1-KP3b Alb	2-KP33d Kspar	3-KP40b Frich	4-KP57a Arfv	5-KP58c Hed	6-KPI3c Aegir	7-KP58a Chl	8-KP33g Astr	9-KP42f Aenig	10-KP42d Titan
SiO ₂	68.25	63.97	46.91	50.1	48.99	51.9	42.85	34.87	40.05	30.33
TiO ₂	0.02	0	0.95	2.21	0.19	3.65	0.01	11.26	8.2	37.81
Al ₂ O ₃	19.44	17.07	1.55	0.29	0.17	0.22	4.35	0.41	0.67	0.55
Fe ₂ O ₃	0	0	0	0	0	25.92	0	0	0	0
FeO	0.51	1.32	35.91	32.1	30.23	3.8	35.32	34.39	42.83	0.06
MnO	0	0	0.87	0.81	0.84	0.29	1.62	2.69	0.94	0
MgO	0.01	0	0.78	0.13	0.69	0.02	0.53	0.02	0.04	0
CaO	0.03	0	5.44	0.59	16.09	0.9	0.46	1.26	0.54	27.87
Na ₂ O	11.67	0.41	4.1	8.72	3.04	12.94	0.1	2.07	7.1	0.15
K ₂ O	0.06	16.75	0.85	1.77	0.02	0.02	0.63	5.97	0.03	0.06
H ₂ O	0	0	1.63	1.09	0	0	11.17	—	0	—
F	0	0	0.41	1.61	0	0	0	1.21	0	0.43
F=O	0	0	-0.18	-0.72	0	0	0	-0.54	0	-0.19
Total	99.99	99.52	99.22	98.70	100.26	99.66	97.04	93.61	100.40	97.07
Si	11.96	12.02	7.69	8.12	1.97	2	9.52	7.92	5.8	4.08
Ti	0	0	0.12	0.27	0.01	0.11	0	1.92	0.9	3.82
Al	4.02	2.78	0.3	0.06	0.01	0.01	1.14	0.1	0.12	0.08
Fe ⁺³	0	0	0	0	0	0.75	0	0	0	0
Fe ⁺²	0.08	0.2	4.92	4.35	1.02	0.12	6.56	6.52	5.2	0
Mn	0	0	0.12	0.11	0.03	0.01	0.3	0.52	0.12	0
Mg	0	0	0.19	0.03	0.04	0	0.18	0	0	0
Ca	0	0	0.96	0.1	0.69	0.04	0.1	0.3	0.08	4.02
Na	3.96	0.14	1.3	2.74	0.24	0.97	0.04	0.92	2	0.04
K	0.02	4.02	0.18	0.37	0	0	0.18	1.72	0	0.02
OH	0	0	1.79	1.18	0	0	16	—	0	—
F	0	0	0.21	0.82	0	0	0	0.43	0	0.09

The structural formulae are calculated on the following basis: albite (Alb) and K-feldspar (Kspar)—32(O); ferrichterite (Frich) and arfvedsonite (Arfv)—24(O, OH, F); hedenbergite (Hed) and aegirine (Aegir)—6(O); chlorite (Chl)—28(O), astrophyllite (Astr)—28.5(O); aenigmatite (Aenig)—20(O); and, titanite (Titan)—20(O, OH, F).

variable size and minute groundmass grains in the felsic ash-flow tuffs (subunits 5a to d). Rarely, amphibole occurs as a thin rim surrounding a clinopyroxene core. The amphibole exhibits a wide range of composition (Table 1) from ferrichterite (sodic-calcic amphibole), to end-member arfvedsonite (alkali amphibole), displaying a continuous trend (Figure 5). This is typical of the amphibole evolutionary trend in anorogenic complexes (e.g., Abdel-Rahman, 1987). Riebeckite is absent.

Compositional zonation of single grains from sodic-calcic cores to sodic rims suggests that the process of fractional crystallization played a significant role during the formation of the amphibole. Most oikocrystic varieties in some banded ash-flow tuffs (subunit 5d), however, are arfvedsonitic (sodic) compositions. Progressive enrichment of Na in late stage melt (due to fractionation and/or vapour-phase transfer of Na at the late magmatic stage) have resulted in a sodium-volatile-rich residual melt from which oikocrystic arfvedsonite has crystallized. Thus, the alkali amphibole in these units is of late magmatic origin, formed from fluid-rich residual melts, and is not a secondary mineral. No evidence was found to support the subsolidus hydrothermal origin of

these amphiboles as suggested by Strong and Taylor (1984). Subsidiary hydrothermal activity, however, resulted in the turbidity of the feldspars, and the formation of secondary minerals such as chlorite-smectite and sericite (see below). Biotite, mostly of annitic composition, is rarely present in similar peralkaline complexes (Abdel-Rahman, 1994); however, no biotite has been observed in rocks of the KPC.

The turbidity of the feldspars and the partial alteration of some alkali amphiboles and pyroxenes to chlorite are due to a subsolidus hydrothermal event. Chlorite is reddish, and has a composition typical of iron-rich, interstratified chlorite-smectite (Table 1), characteristic of chlorites in peralkaline rocks (Abdel-Rahman, 1995). Accessory minerals include zircon, apatite, deep-reddish aenigmatite, titanite and orange to golden-yellow astrophyllite occurring in association with the ferromagnesian minerals. The compositions of some of these accessory phases are also given in Table 1.

GEOCHEMISTRY

Table 2 lists the average geochemical analyses (see Saunders, 1994) of the major units found in the KPC. These

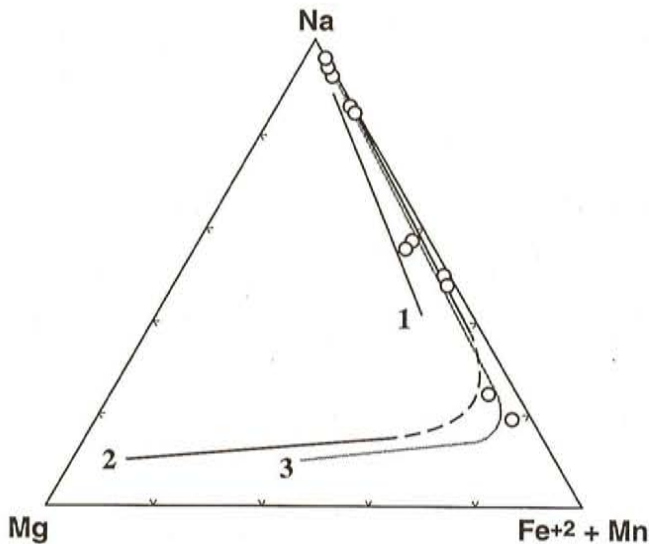


Figure 4. Na-Mg-(Fe⁺²+Mn) triangular diagram showing the compositional trend of the pyroxenes. Curves labeled 1 and 2 represent the trend of pyroxenes from undersaturated alkaline complexes of the Cretaceous North Pyrenean rift zone (after Azambre *et al.*, 1992); curve 3 represents the trend of pyroxenes from peralkaline granites and syenites of the Mulanje complex, Malawi (after Platt and Woolley, 1986).

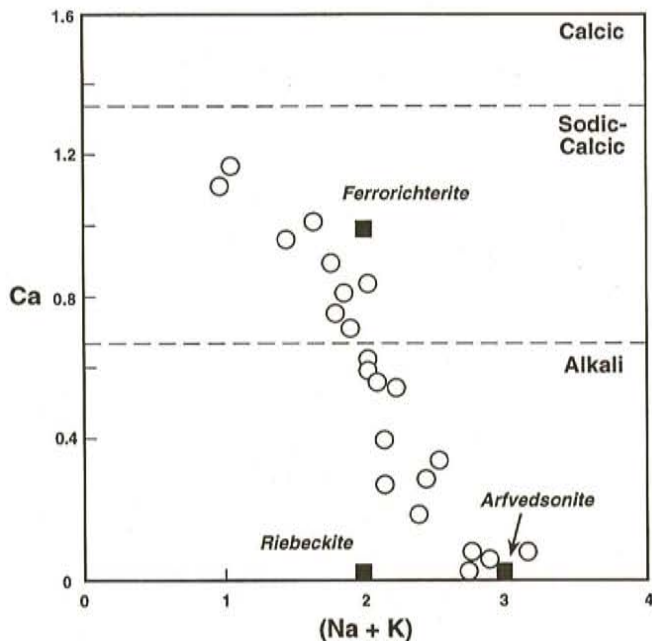


Figure 5. Plot of (Na+K) vs Ca (ions per unit cell) for amphiboles from the King's Point complex. Black boxes represent end-member compositions; note the continuous trend from ferrichterite to arfvedsonite.

data indicate that a few units (subunits 5b and parts of 5d) are peralkaline, as indicated by apfatic index (molecular K_2O+Na_2O/Al_2O_3) values >1.0 , whereas others are transitional or subalkaline (Unit 4 and subunits 5a,c; A.I.

0.85–1.0). However, petrographic and mineralogical data indicate that feldspars and some mafic minerals are altered, suggesting that some post-deposition subsolidus alteration occurred. Comparison of average data for unaltered and altered members of subunit 5d (Table 2; analyses 9 and 10) indicates that alkali depletion occurred in some volcanic rocks; therefore, A.I. values do not always reflect magmatic compositions. The A.I. vs Zr/Al plots are used here to illustrate depletion of Na and K and reduction of A.I. in subunit 5d during hydrothermal alteration (Figure 6). A similar, but more intense, process occurred in peralkaline ash-flow tuffs of the Flowers River cauldron complex (Figure 6; Abdel-Rahman and Miller, 1994; Miller 1994; R.R. Miller and A.M. Abdel-Rahman, unpublished data.). It is tentatively inferred that Na and perhaps K depletion in Unit 5 and probably Unit 4 results in low A.I. values (i.e., subalkaline compositions) of initially peralkaline rocks.

Figure 7 illustrates the relationships between pairs of incompatible elements in the KPC (Zr vs. Nb; Zr vs. Y). Collinear arrays in these two diagrams for all members of the KPC, except Unit 2, suggest cogenetic and possibly comagmatic relationships among these units. Unit 2 appears to be unrelated to other members of the KPC; thus, it probably belongs to an early volcanic suite of different origins.

Units of the KPC plot in the within-plate-granite field (WPG) of a tectonic discrimination diagram for granitoid rocks (Y vs. Nb, Figure 8a; Pearce *et al.*, 1984) and in the A-type field of a genetic or source discrimination diagram (Ga/Al vs. Zr, Figure 8b; Whalen *et al.*, 1987a). An incompatible ratio diagram (Figure 9a; Eby, 1992) determines that the KPC belongs to the A2 granitoid subgroup. This subgroup characterizes rocks with a source that lies between values characteristic of continental crust and island arc basalts. Figure 9b, which combines the Y/Nb data of Eby (1992) and the Zr/Nb data of Leat *et al.* (1986), verifies that the KPC belongs to the A2 granitoid subgroup and that it exhibits the characteristics of source rocks previously affected by subduction or continent collision magmatic processes.

Figure 10, which is a Pearce element ratio modification (R.R. Miller and A.M. Abdel-Rahman, unpublished data) of the Macdonald diagram (Macdonald, 1974), verifies that Unit 4 and all members of Unit 5 are peralkaline rocks; furthermore, it indicates that all members of Unit 5 are comendites. This diagram uses only conserved elements (Al, Zr and Fe) to screen out the effects of hydrothermal depletion of alkali elements.

DISCUSSION

ORIGIN OF PERALKALINITY IN THE VOLCANIC ROCKS

Both Kontak and Strong (1986) and Mercer *et al.* (1985) suggest that the peralkalinity of Unit 5 occurs due to metasomatic processes connected to the mildly peralkaline feldspar-porphyrific syenite (Unit 4) and possible intrusive equivalents of subunit 5c (quartz-feldspar±amphibole-

Table 2. Geochemical data (averages) for major units of the Kings Point complex

Sample No.	1	2	3	4	5	6	7	8	9	10	11	12
Rock type	QF AF	Aph. AF	Syenite	AF	Aph. AF	FQ AF	Granite	Q Syenite	R Spot AF	A AF	A AF (alt.)	Granite
Unit	Unit 2	Unit 3	Unit 4	Subunit 5a	Subunit 5b	Subunit 5c	Subunit 5c	Subunit 5c	Subunit 5d	Subunit 5d	Subunit 5d	Unit 6
N	Ave (4)	Ave (6)	Ave (23)	Ave (5)	Ave (6)	Ave (29)	Ave (15)	Ave (5)	Ave (13)	Ave (19)	Ave (5)	Ave (13)
SiO ₂	77.63	76.94	66.91	77.37	76.43	74.91	75.61	73.90	75.61	75.51	76.14	74.83
TiO ₂	0.08	0.16	0.89	0.17	0.17	0.24	0.21	0.27	0.18	0.18	0.18	0.24
Al ₂ O ₃	12.16	11.68	13.07	10.94	10.73	11.75	11.50	12.15	10.57	10.57	10.63	12.86
Fe ₂ O ₃	0.94	1.35	3.24	1.91	2.30	1.74	1.54	2.15	2.31	1.83	2.89	0.68
FeO	0.35	0.52	2.36	0.75	1.18	1.13	1.24	0.82	1.49	1.95	0.83	0.89
MnO	0.02	0.03	0.12	0.04	0.04	0.05	0.05	0.05	0.05	0.05	0.04	0.03
MgO	0.29	0.12	0.91	0.17	0.06	0.14	0.09	0.22	0.07	0.05	0.10	0.27
CaO	0.33	0.16	1.88	0.11	0.15	0.29	0.17	0.47	0.23	0.14	0.37	0.55
Na ₂ O	2.65	2.13	4.54	3.68	3.79	3.58	3.89	4.03	4.08	4.30	3.73	3.82
K ₂ O	4.12	5.24	3.88	3.69	4.41	4.93	4.38	4.69	4.20	4.46	3.79	4.71
P ₂ O ₅	0.01	0.02	0.25	0.02	0.02	0.03	0.02	0.04	0.01	0.01	0.00	0.04
F	0.04	0.03	0.07	0.03	0.05	0.02	0.01	0.02	0.04	0.05	0.01	0.03
H ₂ O+	0.83	0.55	1.01	0.52	0.34	0.63	0.53	0.63	0.28	0.34	0.47	0.68
H ₂ O-	0.20	0.19	0.39	0.21	0.31	0.27	0.23	0.29	0.17	0.19	0.37	0.34
CO ₂	0.22	0.11	0.47	0.08	0.08	0.15	0.10	0.26	0.08	0.10	0.37	0.11
S	0.02	0.21	0.01	0.16	0.01	0.03	0.01	0.01	0.02	0.01	0.01	0.01
A.I.	0.73	0.79	0.89	0.92	1.03	0.96	0.97	0.96	1.07	1.13	0.96	0.89
Cu	18	9	8	16	10	7	9	9	16	18	9	7
Pb	6	22	8	8	22	10	12	9	27	30	23	10
Zn	36	52	121	69	144	89	93	94	210	231	188	29
Ni	7	1	4	6	2	3	4	3	2	3	1	3
Sc	8.4	3.7	9.0	1.2	0.5	1.5	0.9	2.0	0.1	0.2	0.1	3.2
Ga	21	19	29	25	32	27	28	26	34	34	34	17
Nb	28	16	25	30	55	28	32	26	67	64	71	12
Zr	121	352	524	640	1344	522	612	489	1522	1544	1522	189
Y	51	48	66	76	145	67	67	59	161	161	166	28
Ce	59	129	128	132	242	150	152	144	241	235	245	71
U	5	6	4	7	11	4	5	4	10	10	10	5
Th	19	13	9	17	29	12	13	12	30	26	36	20
Sr	42	35	123	17	16	26	14	27	8	6	11	69
Rb	155	158	80	93	210	104	103	104	175	202	132	154
Ba	124	606	426	227	28	272	106	301	23	12	39	473
FeOt/Zr (mol.)	144.9	72.4	143.5	56.6	34.9	74.3	61.0	82.8	33.7	32.6	33.5	109.9
Al ₂ O ₃ /Zr (mol.)	897.4	296.6	223.0	152.9	71.4	201.5	168.0	222.3	62.1	61.3	62.5	608.9

Trace elements in ppm; ICP-ES and AAS analysis, Newfoundland Geological Survey Branch Lab.; U by INAA; F by specific ion electrode. Major elements in wt.%; ICP-ES analysis, Newfoundland Geological Survey Branch Lab.; CO₂, S and H₂O+ by IR analysis. See Hayes (1994) for analytical techniques and analytical accuracy. FeOt = total Fe as FeO. AF = ash flow; Q = quartz; F = feldspar; A = amphibole; aph. = aphyric; R = red; Fg-Mg = fine/medium-grained.

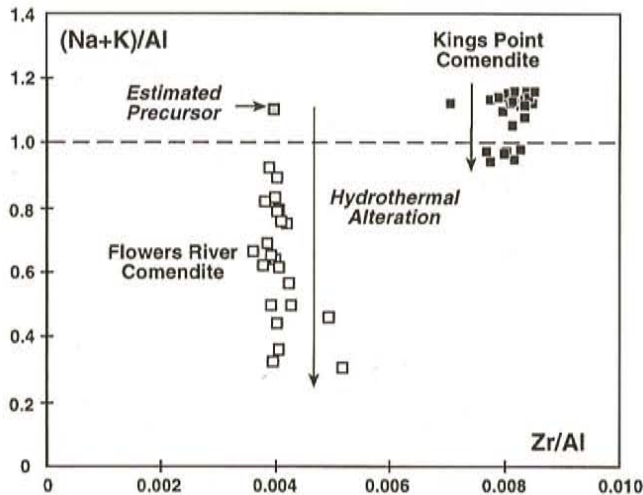


Figure 6. The effect of hydrothermal alteration on peralkaline ash-flow tuffs of the King's Point complex and comparison with the Flowers River cauldron complex. Note that the y-axis is the peralkaline or agpaite index and the x-axis represents conserved or immobile elements. Hydrothermal alteration causes alkali-loss relative to alumina resulting in reduction of the peralkaline index. Comendite from the Flowers River cauldron complex (R.R. Miller and A.M. Abdel-Rahman, unpublished data) illustrates extreme alkali-loss, whereas the King's Point comendite (individual samples) shows relatively minor loss; however, peralkaline rocks from both complexes exhibit peralkaline values less than one.

porphyritic granite and quartz syenite; Table 2). This interpretation is not supported here, instead the following conclusions are presented to substantiate a magmatic vs. metasomatic origin for peralkalinity in the KPC: 1) peralkaline ash-flow tuffs in subunit 5b and peralkaline amphibole-porphyritic rocks in subunit 5d exhibit consistent conserved element geochemical values over large thicknesses (up to 300 m) and over long strike distances (Figure 1); these results are unlikely during contact metasomatic processes; 2) amphibole and pyroxene data (Table 1, Figure 4) indicate magmatic trends consistent with magmatic peralkaline complexes; 3) amphibole-bearing ring dykes, particularly in the Middle Arm Point area, are younger than possible metasomatizing intrusive rocks; 4) crosscutting alkali-rich hydrothermal veins and associated rare-metal mineralization are absent from the KPC; 5) Zr, Y, Nb and Al exhibit relationships of conserved or immobile elements (e.g., Figures 6 and 7), whereas a metasomatic origin demands mobility for these elements; 6) the lack of a continuum of chemical data (e.g., Zr in Figure 7) between peralkaline (Unit 5) and non-peralkaline volcanic rocks (Unit 3) is inconsistent with metasomatic processes; and, 7) geochemical data indicate (e.g., Figures 6 and 8) that the KPC peralkaline rocks exhibit compositions similar to known recent magmatic rocks. In conclusion, these observations suggest that metasomatic textures observed in the KPC (Kontak and Strong, 1986; Strong and Taylor, 1984) result from post-depositional alkali-depletion that produced a decrease of peralkalinity (s.s.).

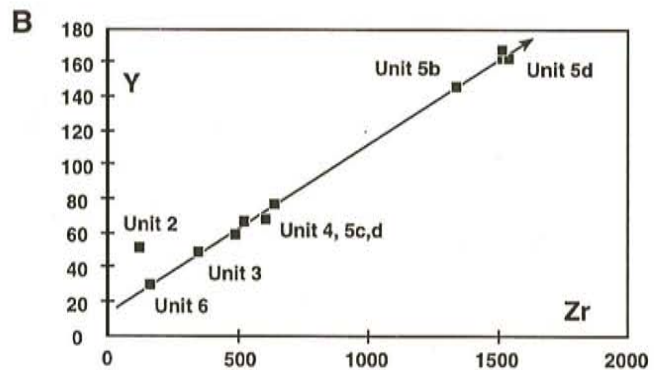
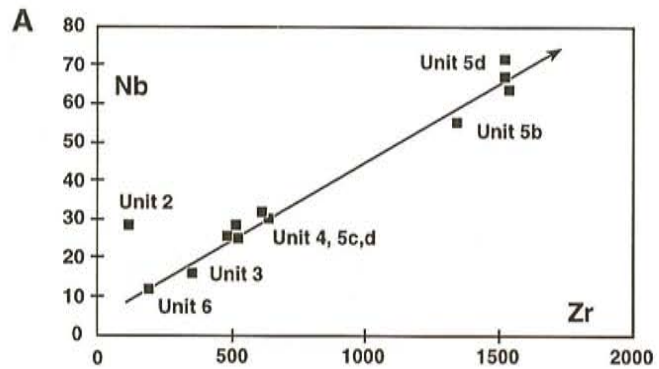


Figure 7. Test for immobile elements and comagmatic relationships in the King's Point complex: A—Zr vs Nb, B—Zr vs Y. Units 3 to 6 exhibit comagmatic relationships, whereas, Unit 2 exhibits the opposite. The linear array observed among rocks of the King's Point complex indicate that Nb, Zr and Y are immobile. Data points represent average data from Table 2.

RARE-METAL MINERALIZATION

This study confirms that the KPC is an intrusive–extrusive, mainly peralkaline complex having many of the parameters of a good rare-metal target. However, extensive lithochemical data from the KPC (Table 2) indicate that high concentrations of rare-metals are unlikely at the present level of erosion.

Rare-metal mineralization in Labrador and elsewhere (Miller 1991, 1992; R.R. Miller and A.M. Abdel-Rahman, unpublished data; Figure 10; Table 3) commonly occurs in pantelleritic volcanic rocks and their intrusive equivalents. The comenditic character of the KPC (compare Tables 2 and 3) suggests initially low concentrations of rare metals in the subvolcanic parent magma chamber; thus, inefficient rare-metal concentration processes or an inadequate period of concentration resulted in relatively rare-metal poor comenditic volcanic rocks and ring dykes. Absence of evidence for low volume ash-flow tuffs or ring dykes, similar to the Flowers River cauldron complex (R.R. Miller and A.M. Abdel-Rahman, unpublished data) and other rare-metal

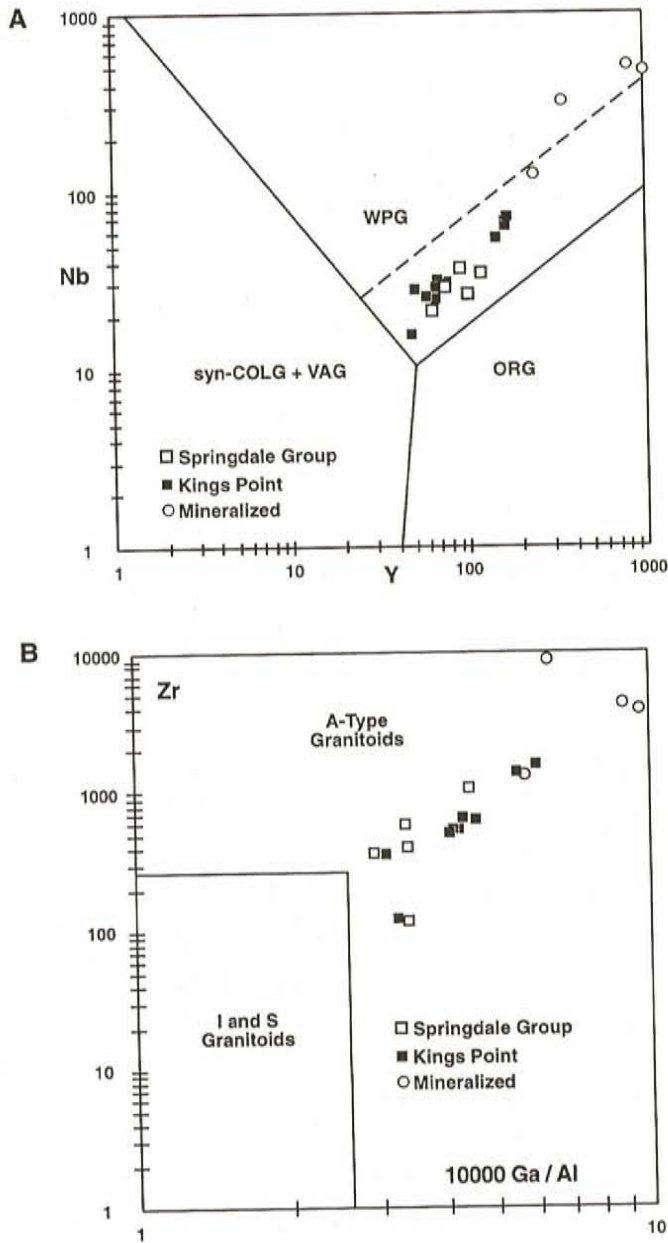


Figure 8. a) Nb–Y tectonic discrimination diagram for granitic rocks (after Pearce et al., 1984). VAG, volcanic-arc granite; syn-COLG, syn-collision granite; ORG, ocean-ridge granite; WPG, within-plate granite. The King’s Point complex, Springdale Group and examples of mineralized peralkaline rocks (Tables 2 and 3) occur in the WPG granite field. b) Zr vs Ga/Al genetic discrimination diagram for granitoids (after Whalen et al., 1987a). The King’s Point complex, Springdale Group and examples of mineralized peralkaline rocks (Tables 2 and 3) occur in the A-type granite field.

mineralized complexes, further lowers the potential for the KPC.

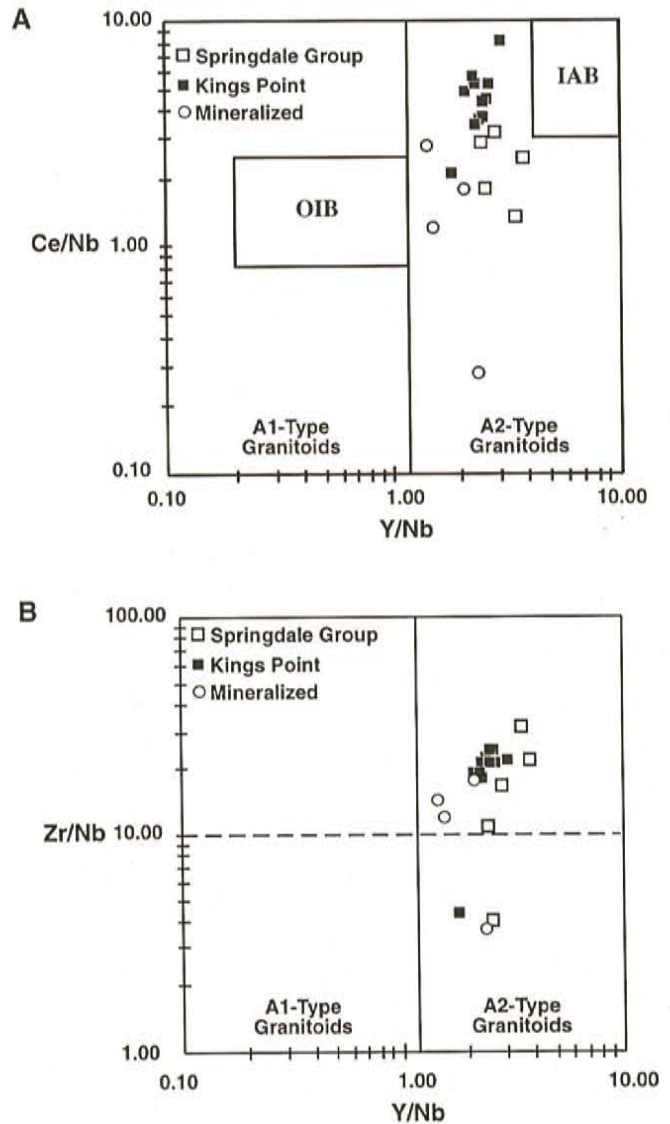


Figure 9. a) Ce/Nb vs Y/Nb discrimination diagram for A-type granitoids (after Eby, 1990, 1992); A1-type granitoids plot in or near the ocean island basalt field (OIB) having Y/Nb values less than 1.2, whereas A2-type granitoids plot in the island-arc basalt (IAB) field or between the OIB and IAB fields, having Y/Nb greater than 1.2. The King’s Point complex, Springdale Group and examples of mineralized peralkaline rocks occur (Tables 2 and 3) in the A2 granitoid field indicating a probable crustal source that previously produced continent-continent collision or island-arc magmatism (Eby, 1992). b) Zr/Nb vs Y/Nb discrimination diagram for A-type granitoids. Combines the Y/Nb discriminator for A1- and A2-type granitoids from Figure 9a (Eby, 1992) with the Zr/Nb discriminator for ocean island/continental rift peralkaline volcanic rocks (Zr/Nb less than 10) and subduction zone related peralkaline volcanic rocks (Zr/Nb greater than 10). A-type rocks related to subduction zone magmatism will occur in the upper right quadrant and ocean island/continental rift related rocks will occur in the lower left quadrant. The King’s Point complex, Springdale Group and examples of mineralized peralkaline rocks (Tables 2 and 3) mainly occur in the upper right quadrant; Unit 2 from the KPC, the low-Zr rhyolite from the Springdale Group and the highly differentiated exotic-rich phase of the Strange Lake peralkaline complex are anomalous.

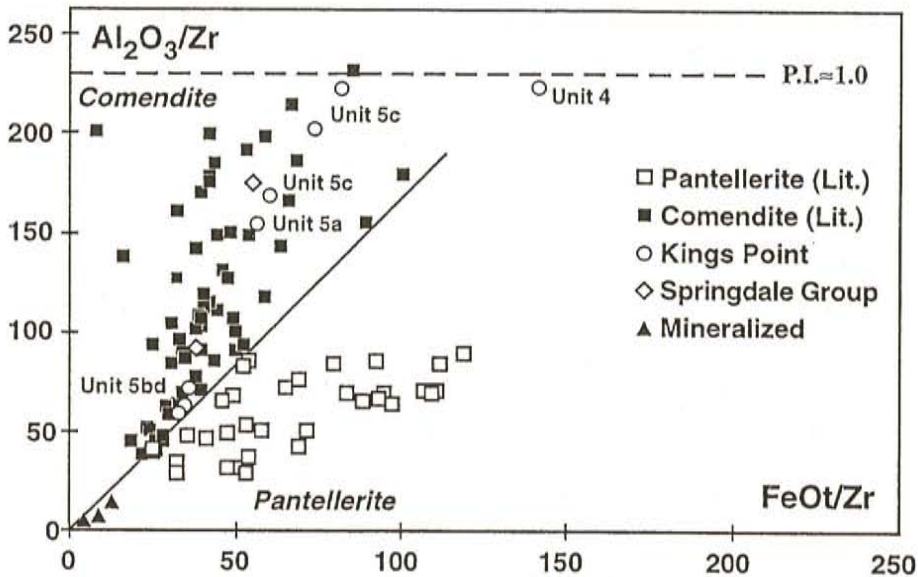


Figure 10. Comendite-pantellerite peralkaline rock differentiation diagram. Molar $\text{Al}_2\text{O}_3/\text{Zr}$ vs. $\text{FeO}_{\text{total}}/\text{Zr}$ —modified from Macdonald (1974) using Pearce Element Ratio theory (e.g., Stanley and Madeisky, 1994) to eliminate the effects of metasomatic alteration. Literature data are from the references in Macdonald (1974) with additional data from Barberi et al. (1975), Noble and Parker (1974), Baker and Henage (1977), Civetta et al. (1984), Macdonald et al. (1987) and Schuraytz et al. (1989). The line $P.I. \approx 1.0$ (peralkaline index) roughly separates data from the literature compilation based on peralkaline index and approximates $\text{Zr} \approx 500$ ppm (higher Zr plots below

the line); Leat et al. (1986) recommend $\text{Zr} \approx 500$ ppm to separate peralkaline from subalkaline rocks. Only data from Unit 5 and Unit 4 of the KPC plot in the peralkaline field (Tables 2 and 3); all others are subalkaline if Zr, Al, and Fe are conserved elements. All Unit 5 data plots in the comendite field.

THE KPC AND THE SPRINGDALE GROUP

Several authors (Coyle and Strong, 1987; Whalen, 1989) suggest a close genetic relationship between the KPC and members of the Springdale Group based on geochemistry, geochronology and spatial relationships. Comparison of geochemical averages for units of the KPC and some averages from the Springdale Group (Tables 2 and 3) indicate several similarities when differences caused by alkali-depletion are considered: 1) Unit 2 (KPC) and low Zr rhyolite from the Springdale Group are basically identical; 2) Unit 3 (KPC) and intermediate Zr rhyolite from the Springdale area (Coyle and Strong, 1987) are very similar, and both have many similarities to the average of Springdale Group volcanic rocks in the Topsails Complex area (Whalen, 1989); 3) Subunit 5a (KPC) and high Zr rhyolite from the Springdale Group are very similar; and 4) Subunits 5b and d (KPC) and peralkaline rocks from the Springdale Group (Sheffield Lake area; Coyle et al., 1986) have several similarities. These data also support a close genetic relationship between these rocks.

Coyle and Strong (1987) postulate that the Springdale Group high silica rhyolites (Table 3), compared above, are out-flow deposits of the KPC. However, the restricted distribution of Unit 3 and the apparent thinness of Unit 2 (subalkaline high-silica rhyolites) in the KPC indicate that they are more likely outflow deposits of another yet unidentified caldera. Peralkaline rocks in the Sheffield Lake area are probably the faulted southeastern portion of the KPC. Minor occurrences of high Zr rhyolite in the Springdale Group may be outflow deposits of the KPC.

The KPC represents a more highly evolved magma than the Springdale Group as it dominantly consists of peralkaline felsic rocks, whereas the Springdale Group mostly consists

of subalkaline felsic volcanic rocks, abundant sedimentary rocks and extensive units of mafic volcanic rocks.

CONCLUSIONS

The following conclusions from this ongoing study of the King's Point complex are made:

- 1) the rare-metal potential is very low when compared to other peralkaline rocks, such as the Flowers River cauldron complex and the Strange Lake peralkaline complex;
- 2) the peralkalinity of the volcanic and plutonic rocks of the complex is a magmatic feature;
- 3) subsolidus alkali-depletion of originally peralkaline precursor volcanic rocks produced subalkaline derivatives;
- 4) several units in the KPC geochemically correlate with high silica rhyolites of the Springdale Group; these units probably represent outflow deposits of the Springdale Caldera;
- 5) the KPC is dominantly a peralkaline volcanic-subvolcanic complex that sits on and intrudes volcanic rocks of the Springdale Group (Units 2 and 3); and
- 6) felsic, subalkaline granitic intrusions (Unit 6) are probably related to later movements on the Green Bay fault, and are unrelated to the peralkaline rocks.

Table 3. Geochemical data from the Springdale Group and some peralkaline rocks

	*Springdale			Springdale Group—High-Si Rhyolites			Micmac Lake		Flowers River		Cross Hills		Strange Lake	
	Ave (7)	Low Zr Ave (3)	Interm. Zr Ave (8)	High Zr Ave (29)	Peralkaline Ave (3)	AF ML90-4	AF ML90-5	A AF Ave (18)	Mineral. Ave (6)	Fg. Gran. Ave (4)	Mineral. Aplite	Ex-poor Ave (61)	Exotic Ave (22)	Ex-rich Ave (14)
SiO ₂	77.66	76.33	76.99	77.07	77.80	76.60	76.45	73.75	76.46	76.42	78.55	70.93	71.58	68.25
TiO ₂	0.12	0.07	0.15	0.16	0.21	0.18	0.17	0.27	0.35	0.14	0.37	0.23	0.36	0.48
Al ₂ O ₃	11.66	11.67	11.86	11.17	10.87	10.87	10.78	9.90	7.82	10.99	7.43	11.29	8.86	7.15
Fe ₂ O ₃	1.13	1.40	1.93	2.24	2.87	2.39	2.43	3.88	1.80	2.61	5.37	2.29	3.92	3.17
FeO	0.57	-	-	-	-	0.19	1.27	1.99	6.10	0.55	0.63	2.33	1.64	1.22
MnO	0.02	0.02	0.02	0.04	0.12	0.06	0.05	0.08	0.08	0.08	0.12	0.10	0.15	0.16
MgO	0.05	0.40	0.17	0.13	0.09	0.43	0.18	0.04	0.10	0.04	0.28	0.06	0.20	0.57
CaO	0.22	0.22	0.23	0.12	0.03	1.53	0.41	0.20	0.01	0.10	0.01	0.69	1.50	4.25
Na ₂ O	2.86	2.64	3.13	3.37	3.87	1.50	3.86	3.88	0.02	3.57	0.86	5.10	4.04	2.93
K ₂ O	4.98	5.04	4.86	4.41	3.85	3.04	4.18	4.34	1.77	4.37	3.05	4.88	4.12	3.59
P ₂ O ₅	0.01	0.00	0.01	0.02	0.02	0.01	0.01	0.01	0.02	0.01	0.01	0.02	0.04	0.08
F	0.06	-	-	-	-	0.05	0.07	0.19	0.05	0.03	0.01	0.42	0.42	1.52
H ₂ O+	0.50	1.24	0.87	0.79	0.63	1.33	0.15	0.36	2.21	0.30	1.44	0.39	0.52	1.69
H ₂ O-	-	-	-	-	-	0.27	0.33	0.22	0.21	0.19	0.43	-	-	-
CO ₂	0.16	-	-	-	-	1.16	0.37	0.20	0.19	0.07	0.24	0.12	0.10	0.12
S	0.02	-	-	-	-	0.00	0.00	0.02	0.10	0.00	0.00	0.01	0.01	0.01
A.I.	0.87	0.84	0.88	0.92	0.97	0.53	1.01	1.12	0.25	0.96	0.63	1.21	1.25	1.22
Cu	3	6	4	5	2	13	12	13	-	13	58	6	10	10
Pb	10	31	18	33	17	10	25	82	285	14	24	168	277	1281
Zn	43	46	46	65	23	89	219	420	802	138	176	587	959	1120
Ni	-	12	0	1	1	1	2	1	-	0	1	0	0	1
Sc	-	-	-	-	-	2.4	0.1	0.0	<0.1	0.2	0	-	-	-
Ga	21	21	18	20	26	21	34	50	45	33	25	53	51	51
Nb	36	29	22	26	34	25	59	311	701	122	467	487	975	4238
Zr	394	114	361	569	1051	610	1419	3630	9922	1388	8490	4148	11423	15317
Y	90	75	62	99	119	68	158	349	1061	237	1030	821	1554	10591
Ce	104	52	68	65	45	162	247	662	1962	205	842	680	1187	1190
U	5.7	5.7	1.3	7.5	5.7	3.0	9.0	10.4	33.2	11.3	58	19.0	39.3	136.8
Th	22	14	20	20	31	16	16	59	227	52	183	103	198	1701
Sr	20	33	51	27	27	61	15	7	5	14	14	30	77	363
Rb	167	193	136	122	145	75	166	407	227	215	186	746	974	895
Ba	38	119	540	534	151	665	27	21	38	48	135	62	60	213
FeO/Zr (mol.)	58.6	171.0	74.8	55.0	38.2	58.7	35.3	21.9	10.3	31.2	9.8	14.8	6.6	3.9
Al ₂ O ₃ /Zr (mol.)	264.7	912.9	294.2	175.6	92.5	159.4	68.0	24.4	7.1	70.8	7.8	24.4	6.9	4.2

* From Whalen (1989); From Coyle and Strong (1987); Miller and Abdel-Rahman, submitted; all others Miller (unpublished data).
 AF = ash flow; A = amphibole; Fg = fine-grained; Gran = Granite; Mineral. = mineralized; - = not available.
 Ex-poor, Exotic and Ex-rich after Miller (1986); Ex = exotic.

ACKNOWLEDGMENTS

R. Miller acknowledges the help of field assistants, J. Ryan (1990, 1991) and C. Harvey (1992), during the mapping and sampling program. H. Wagenbauer, C. Finch and assistants at the laboratory of the Newfoundland Department of Natural Resources provided geochemical analyses. Continuous support provided by NSERC to A.M. Abdel-Rahman is greatly appreciated. J. Whalen kindly provided a copy of an unpublished GSC Report. Drs. H.S. Swinden and A. Kerr suggested many improvements to an earlier version of the manuscript.

REFERENCES

- Abdel-Rahman, A.M.
1987: Crystallization of amphiboles in the plutonic complexes of northeastern Egypt: Implications for magma evolution. *Neues Jahrbuch Miner. Abh.*, Volume 157, pages 319-335.
- 1992: Mineral chemistry and paragenesis of astrophyllite from Egypt. *Mineralogical Magazine*, Volume 56, pages 17-26.
- 1994: Nature of biotites from alkaline, calc-alkaline, and peraluminous magmas. *Journal of Petrology*, Volume 35, pages 525-541.
- 1995: Chlorites in a spectrum of igneous rocks: mineral chemistry and paragenesis. *Mineralogical Magazine*, Volume 59, pages 129-141.
- Abdel-Rahman, A.M. and Miller, R.R.
1993: The Flowers River anorogenic caldera complex, Labrador: stratigraphy and evolution. *Geological Association of Canada—Mineralogical Association of Canada, Joint Annual Meeting, Abstracts*, Volume 18, page A1.
- 1994: Extreme Na-depletion in peralkaline volcanic rocks of the Flowers River cauldron complex. *Geological Association of Canada—Mineralogical Association of Canada, Joint Annual Meeting, Abstracts*, Volume 19, page A1.
- Azambre, B., Rossy, M. and Albarede, F.
1992: Petrology of the alkaline magmatism from the Cretaceous North-Pyrenean rift zone (France and Spain). *European Journal of Mineralogy*, Volume 4, pages 813-834.
- Baker, B.H. and Henage, L.F.
1977: Compositional changes during crystallization of some peralkaline silicic lavas of the Kenya Rift Valley. *Journal of Volcanology and Geothermal Research*, Volume 2, pages 17-28.
- Barberi, F., Ferrara, G., Santacroce, R., Treuil, M. and Varet, J.
1975: A transitional basalt-pantellerite sequence of fractional crystallization, the Boina Centre (Afar Rift, Ethiopia). *Journal of Petrology*, Volume 16, pages 22-56.
- Batterson, M. and Miller, R.
1987: A new Y-Nb-Be showing in the western part of the Central Mineral Belt, Labrador. Newfoundland Department of Mines, Mineral Development Division, [Open File 13L/1 (66), 5 pages].
- Cawood, P.A. and Dunning, G.R.
1993: Silurian age for movement on the Baie Verte Line: Implications for accretionary tectonics in the Northern Appalachians. *Geological Society of America, Abstracts with Programs*, Volume 25, no. 6, page A422.
- Civetta, L., Cornette, Y., Crisci, G., Gillot, P.Y., Orsi, G. and Requejo, C.S.
1984: Geology, geochronology and chemical evolution of the Island of Pantelleria. *Geological Magazine*, Volume 121, pages 541-562.
- Chandler, F.W., Sullivan, R.W. and Currie, K.L.
1987: The age of the Springdale Group, western Newfoundland, and correlative rocks—evidence for a Llandovery overlap assemblage in the Canadian Appalachians. *Transactions of the Royal Society of Edinburgh: Earth Sciences*, Volume 78, pages 41-49.
- Coyle, M.
1990: Geology, geochemistry and geochronology of the Springdale Group, an early Silurian caldera in central Newfoundland. Unpublished Ph.D. thesis, Memorial University of Newfoundland, St. John's, Newfoundland.
- Coyle, M. and Strong, D.F.
1987: Geology of the Springdale Group: a newly recognized Silurian epicontinental-type caldera in Newfoundland. *Canadian Journal of Earth Sciences*, Volume 24, pages 1135-1148.
- Coyle, M., Strong, D.F. and Dingwell, D.B.
1986: Geology of the Sheffield Lake group, west-central Newfoundland. *In Current Research, Part A. Geological Survey of Canada, Paper 86-1A*, pages 455-459.
- Eby, G.N.
1990: The A-type granitoids: A review of their occurrence and chemical characteristics and speculations on their petrogenesis. *Lithos*, Volume 26, pages 115-134.
- 1992: Chemical subdivision of the A-type granitoids: Petrogenetic and tectonic implications. *Geology*, Volume 20, pages 641-644.

- Fryer, B.J., Kerr, A., Jenner, G.A. and Longstaffe, F.J.
1992: Probing the crust with plutons: regional isotopic geochemistry of granitoid intrusions across insular Newfoundland. *In* Current Research. Newfoundland Department of Mines and Energy, Geological Survey Branch, Report 92-1, pages 119-139.
- Hayes, J.P.
1994: Analytical accuracy: a review of analyses of the standards SY-2 and MRG-1 from departmental records. *In* Current Research. Newfoundland Department of Mines and Energy, Geological Survey Branch, Report 94-1, pages 117-134.
- Hibbard, J.
1983: Geology of the Baie Verte Peninsula, Newfoundland. Newfoundland Department of Mines and Energy, Mineral Development Division, Memoir 2, 279 pages.
- Kontak, D.J. and Strong, D.F.
1986: The volcano-plutonic King's Point complex, Newfoundland. *In* Current Research, Part A. Geological Survey of Canada, Paper 86-1A, pages 465-470.
- Leat, P.T., Jackson, S.E., Thorpe, R.S. and Stillman, C.J.
1986: Geochemistry of bimodal basalt-subalkaline/peralkaline rhyolite provinces within the southern British Caledonides. *Journal of the Geological Society*, London, Volume 143, pages 259-273.
- Macdonald, R.
1974: Nomenclature and petrochemistry of the peralkaline oversaturated extrusive rocks. *Bulletin Volcanology*, Volume 38, pages 498-516.
- Macdonald, R., Davies, G.R., Bliss, C.M., Leat, P.T., Bailey, D.K. and Smith, R.L.
1987: Geochemistry of high silica peralkaline rhyolites, Naivasha, Kenya Rift Valley. *Journal of Petrology*, Volume 28, pages 979-1008.
- Mercer, B., Strong, D.F., Wilton, D.H.C. and Gibbons, D.
1985: The King's Point Complex, western Newfoundland. *In* Current Research, Part A. Geological Survey of Canada, Paper 85-1A, pages 737-741.
- Miller, R.R.
1986: Geology of the Strange Lake alkalic complex and the associated Zr-Y-Nb-Be-REE mineralization. *In* Current Research. Newfoundland Department of Mines and Energy, Mineral Development Division, Report 86-1, pages 11-19.
1987: The relationship between Mann-type Nb-Be mineralization and felsic peralkaline intrusives, Letitia Lake Project, Labrador. *In* Current Research. Newfoundland Department of Mines and Energy, Mineral Development Division, Report 87-1, pages 83-91.
1988: Yttrium (Y) and other rare metals (Be, Nb, Ta, Zr) in Labrador. *In* Current Research. Newfoundland Department of Mines, Mineral Development Division, Report 88-1, pages 229-245.
1989: Rare-metal targets in insular Newfoundland. *In* Current Research. Newfoundland Department of Mines and Energy, Geological Survey Branch, Report 89-1, pages 171-179.
1991: Preliminary evaluation of rare-metal targets in insular Newfoundland. *In* Current Research. Newfoundland Department of Mines and Energy, Geological Survey Branch, Report 91-1, pages 327-334.
1992: Preliminary report of the stratigraphy and mineralization of the Nuiklavik volcanic rocks of the Flowers River Igneous Suite. *In* Current Research. Newfoundland Department of Mines and Energy, Geological Survey Branch, Report 92-1, pages 251-258.
1993: Geology and rare-metal mineralization of the Nuiklavik volcanic rocks of the Flowers River Igneous Suite, Labrador. *In* Current Research. Newfoundland Department of Mines and Energy, Geological Survey Branch, Report 93-1, pages 363-371.
1994: Extreme Na-depletion in the peralkaline volcanic rocks of the Middle Proterozoic Flowers River cauldron complex, Labrador. *In* Current Research. Newfoundland Department of Mines and Energy, Geological Survey Branch, Report 94-1, pages 233-246.
- Miller, R.R. and Abdel-Rahman, A.M.
1992: Geology and rare-metal mineralization of the Nuiklavik volcanics of the Flowers River Igneous Suite, Labrador. Geological Association of Canada—Mineralogical Association of Canada, Joint Annual Meeting, Wolfville, Abstracts, Volume 17, pages A79.
- Noble, D.C. and Parker, D.F.
1974: Peralkaline silicic volcanic rocks of the western United States. *Bulletin Volcanology*, Volume 38, pages 803-827.
- Pearce, J.A., Harris, N.B.W. and Tindle, A.G.
1984: Trace element discrimination diagrams for tectonic interpretation of granitic rocks. *Journal of Petrology*, Volume 25, pages 956-983.
- Platt, R.G. and Woolley, A.R.
1986: The mafic mineralogy of the peralkaline syenites and granites of the Mulanje complex, Malawi. *Mineralogical Magazine*, Volume 50, pages 85-99.
- Prior, G.J.
1988: Geology and litho-geochemistry of the Kings Point property, Baie Verte Peninsula, Newfoundland. Unpublished report, Teck Exploration Ltd. [12H/9(1076)]

- Saunders, C. (compiler)
1994: Volcanic rock geochemical database. Newfoundland Department of Mines and Energy, Geological Survey Branch, [Open File NFLD/2414 v. 1.0].
- Schuraytz, B.C., Vogel, T.A. and Younker, L.W.
1989: Evidence for dynamic withdrawal from a layered magma body: The Topopah Spring Tuff, southwestern Nevada. *Journal of Geophysical Research*, Volume B94, pages 5925-5942.
- Stanley, C.R. and Madeisky, H.E.
1994: Lithochemical exploration for hydrothermal ore deposits using Pearce Element Ratio Analysis. *In* Alteration and Alteration Processes Associated with Ore-forming Systems. *Edited by* D.R. Lentz. Geological Association of Canada, Short Course Notes, Volume 11, pages 193-211.
- Strong, D.F. and Taylor, R.P.
1984: Magmatic-subsolidus and oxidation trends in composition of amphiboles from silica-saturated peralkaline igneous rocks. *Tschermaks Mineralogische und Petrographische Mitteilungen*, Volume 32, pages 211-222.
- Whalen, J.B.
1989: The Topsails igneous suite, western Newfoundland: an Early Silurian subduction-related magmatic suite? *Canadian Journal of Earth Sciences*, Volume 26, pages 2421-2434.
- Whalen, J.B., Currie, K.L. and Chappell, B.W.
1987a: A-type granites: geochemical characteristics, discrimination and petrogenesis. *Contributions to Mineralogy and Petrology*, Volume 95, pages 407-419.
- Whalen, J.B., Currie, K.L. and van Breemen, O.
1987b: Episodic Ordovician-Silurian plutonism in the Topsails igneous terrane, western Newfoundland. *Transactions of the Royal Society of Edinburgh: Earth Sciences*, Volume 78, pages 17-28.
- Williams, H., Dickson, W.L., Currie, K.L., Hayes, J.P. and Tuach, J.
1989: Preliminary report on a classification of Newfoundland granitic rocks and their relations to tectonostratigraphic zones and lower crustal blocks. *In* Current Research, Part A. Geological Survey of Canada, Paper 89-1B, pages 47-53.

Note: Geological Survey file numbers are included in square brackets.